

10/22/93 YS①

CORF 92 111 72 - 1

# Klystron Equalization for RF Feedback\*

P. Corredoura  
Stanford Linear Accelerator Center, Stanford University, Stanford, CA 94309

## ABSTRACT

The next generation of colliding beam storage rings support higher luminosities by significantly increasing the number of bunches and decreasing the spacing between respective bunches. The heavy beam loading requires large RF cavity detuning which drives several lower coupled bunch modes very strongly. One technique which has proven to be very successful in reducing the coupled bunch mode driving impedance is RF feedback around the klystron-cavity combination. The gain and bandwidth of the feedback loop is limited by the group delay around the feedback loop. Existing klystrons on the world market have not been optimized for this application and contribute a large portion of the total loop group delay. This paper describes a technique to reduce klystron group delay by adding an equalizing filter to the klystron RF drive. Such a filter was built and tested on a 500 kW klystron as part of the on going PEP-II R&D effort here at SLAC.

## 1. INTRODUCTION

The proposed PEP-II B-factory at SLAC centers around a 3.1 GeV positron ring and 9.0 GeV electron ring. Current in the two rings is 2.14 A and 1.48 A respectively. A harmonic number of 3492, RF frequency of 476 MHz, and filling every other bucket allows for 1746 possible bunches in each ring. In order to allow ions to clear in the electron ring, only 1658 buckets are planned to be populated. The number of bunches in the positron ring will be tailored to match transients in the two rings.

The gap in the bunch train introduces strong revolution harmonics to the bunch spectrum. These harmonics are spaced at 136 kHz intervals and interact with the impedance associated with the fundamental accelerating mode of the RF cavities as shown in figure 1. Each revolution harmonic has an upper and lower synchrotron oscillation sideband spaced

7 kHz away. The driving impedance of each coupled bunch mode can be calculated by the difference in the real impedance seen by the upper and lower revolution sideband associated with the mode. Modes are driven if an upper sideband sees a higher real impedance than the lower sideband. Note that an upper sideband may be at a lower frequency than a lower sideband. A good example is the most strongly driven, the -1 mode.

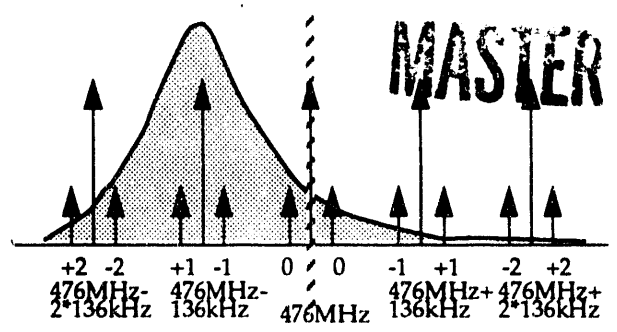


Figure 1: Cavity impedance and beam spectrum with mode numbers of sidebands labeled.

\* Work supported by Department of Energy contract DE-AC03-76SF00515.

Great effort has been devoted to reducing the impedance of higher order cavity modes<sup>1</sup> down to a level where driven coupled bunch

modes can be damped by a wide band digital feedback system.<sup>2,3</sup> Reducing the cavity impedance of the accelerating mode is not an efficient option. One solution is to use RF feedback to reduce the impedance viewed by the beam.

## 2. RF FEEDBACK BASICS

The philosophy behind RF feedback is illustrated in figure 2. A sample of the cavity fields is amplified and phase shifted such that the hybrid summing node takes the difference between the reference and the cavity signal. This error signal is then used to drive the klystron and cavity. Beam induced signals in the cavity appear as an error signal in the loop, are inverted around the loop and canceled in the cavity. These induced signals are reduced by the amount of loop gain at the frequency in question. The gain and bandwidth of the loop is limited by the total group delay around the loop.

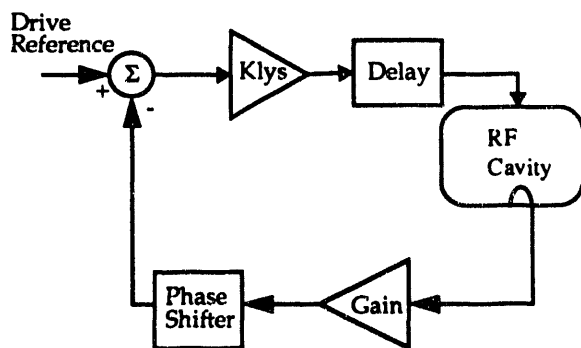


Figure 2: Block diagram of a RF feedback loop.

## 3. TRANSFER FUNCTIONS

### 3.1 Klystron

Using a HP 8753 network analyzer, the transfer function of the 500 kW PEP-II klystron was measured. A linear model was then fit to the response using MATLAB. The

results are plotted in figure 3.

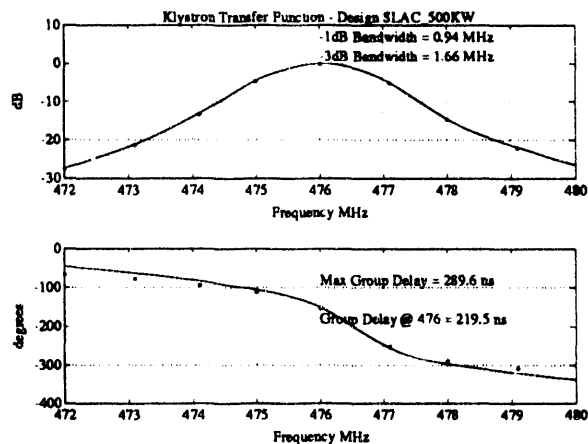


Figure 3: Modeled klystron transfer function

Measured data appear as asterisk while the model fit is the solid line. Note the maximum group delay of ~300 ns. Group delay is defined as the slope of the phase response:

$$t_g = \frac{d\phi}{d\omega}$$

### 3.2 RF Cavity

The bandwidth of the loaded cavity is ~70 kHz. Figure 4 shows the expected 180 degree phase shift through the resonance.

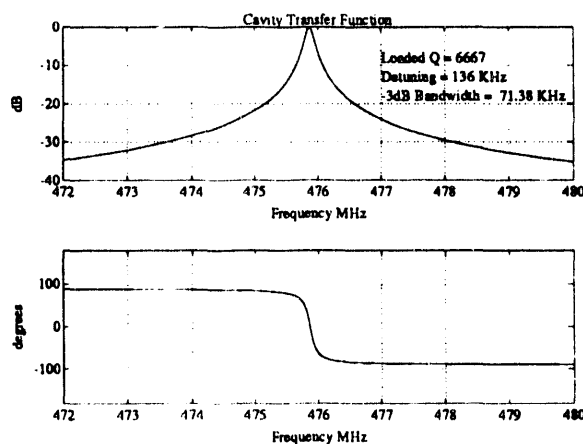


Figure 4: RF cavity transfer function

### 3.3 Transmission Delay

Transmission delay is the lumped effect of coaxial cables and waveguides. In the frequency range we are concerned with, waveguides can be considered frequency independent delay elements. Figure 5 shows the phase response of the 155 ns of delay estimated for PEP-II. Note that this is roughly half the delay associated with the klystron.

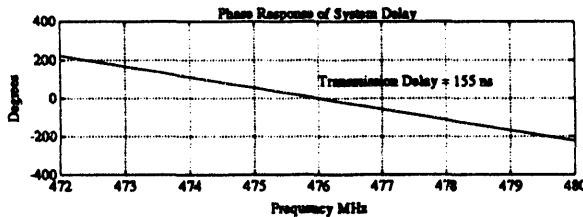


Figure 5: Phase response of transmission delay

### 3.4 Other Elements

The response of the electronic phase shifters manufactured at SLAC have a flat amplitude response and a group delay of ~5 ns. Their contribution was included in the transmission delay of 155 ns.

The gain element is a wide band solid state amplifier which contributes a few ns of group delay to the loop. This was also included in 3.3 above.

### 3.5 Open Loop Response

Combining the individual transfer functions we can calculate the open loop response of the feedback loop. The value of the gain element is determined by stability criteria. Here we have chosen the limit to be a phase margin of relatively conservative 60 degrees.

Figure 6 displays the open loop transfer function. The location of the upper and lower phase margins are shown. If one wanted to

increase the gain and bandwidth of the loop, the total amount of phase shift between the 0 dB points would have to be reduced.

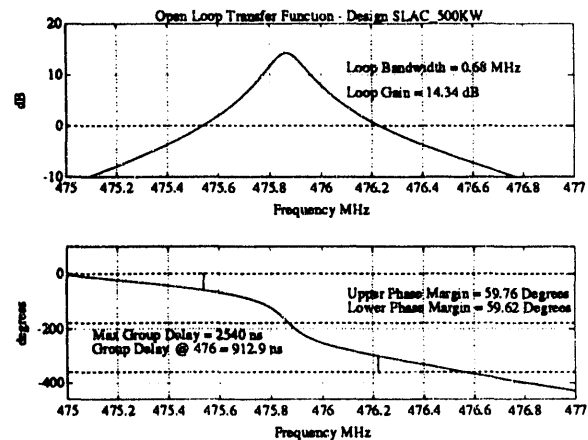


Figure 6: Open loop response

The 180 degree contribution from the cavity occurs over a small bandwidth when compared to the feedback loop bandwidth of ~700 kHz. The RF power is not available to cancel the cavity response, hence this effect is fixed. The transmission delay should be minimized when a system is designed, but is generally not a variable which can be optimized. This leaves us with the klystron. In terms of the "phase budget" we can write:

$$2(P_m) + 180 + 360(t_g \Delta f) + \Delta P_{kly} \leq 360$$

This equation states that the sum of phases required for phase margins (2x60 degrees), cavity resonance (180 degrees), transmission delay, and klystron group delay must remain less than 360 degrees. Since the first two terms are constants, we can state that the sum of the phase contribution of the transmission delay and the klystron group delay must be less than 60 degrees.

One can view the klystron transfer function to be similar to that of a bandpass filter. Increasing the bandwidth of the filter decreases

the group delay. By using the bandpass equivalent of lag-lead compensation on the klystron drive signal, the location of the poles in the klystron transfer function can be spread apart to increase the tube bandwidth. The filter which performs this function is called an equalizer.

#### 4. EQUALIZER DEVELOPMENT

The klystron equalizer is a filter which places emphasis on the klystron drive at frequencies where output has begun to decrease. The design began with generating a linear model for the klystron response. Figure 7 is the output of a MATLAB file which allows the user to interactively fit a model to data measured with a network analyzer.

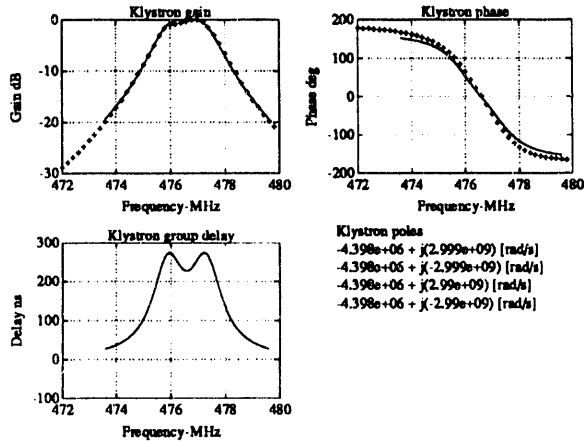


Figure 7: Klystron model development

Next we design a filter transfer function which has zeros to cancel the klystron poles. Poles are selected based on the final combined group delay or bandwidth desired. The goal for our filter was to decrease the group delay by a factor of four. The response of the equalizer filter is plotted in figure 8. Note the positive phase slope which creates a negative group

delay of ~200 ns.

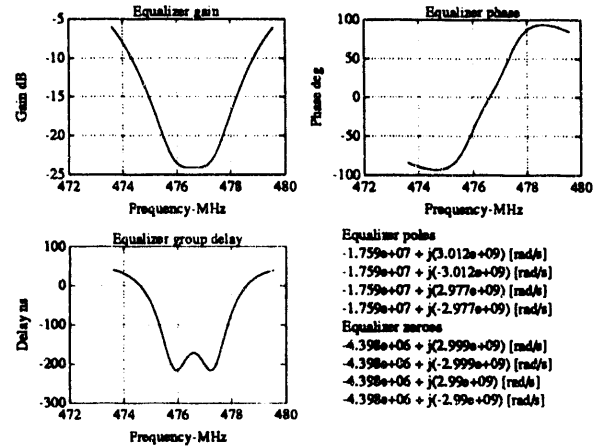


Figure 8: Equalizer response

Placing the new filter in the klystron drive produces a new combined response with a larger bandwidth and smaller group delay. Figure 9 shows the combined response.

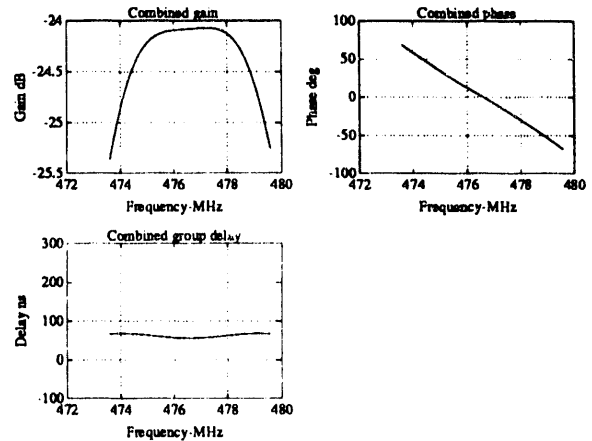


Figure 9: Combined response

#### 5. IMPLEMENTATION

Studying the required poles and zeros of the equalizer shown in figure 8, we observe that the transfer function contains complex zeros. Synthesis of complex zeros is difficult in lumped elements, especially at microwave frequencies. The chosen approach was to mix down to baseband in quadrature, process the signals and then mix back up to 476 MHz.

Figure 10 illustrates this topology.

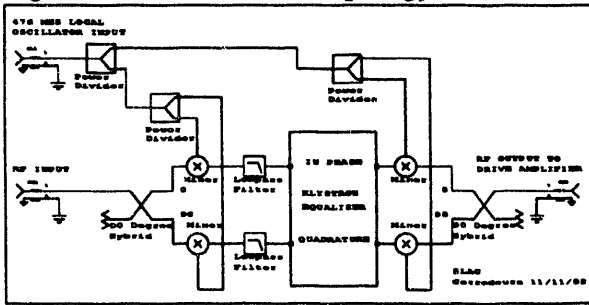


Figure 10: Equalizer block diagram

Using the baseband technique the complexity of the filter is reduced, but two filters are required instead of one. To transform the filter to baseband, 476 MHz is translated to DC, hence the location of the imaginary portion of the complex poles and zeros above 476 MHz are shifted down by 476 MHz. Poles and zeros below 476 MHz are ignored if the filter response is symmetric. This greatly reduces the required Q of the filter. Figure 11 shows the required baseband response of the filter.

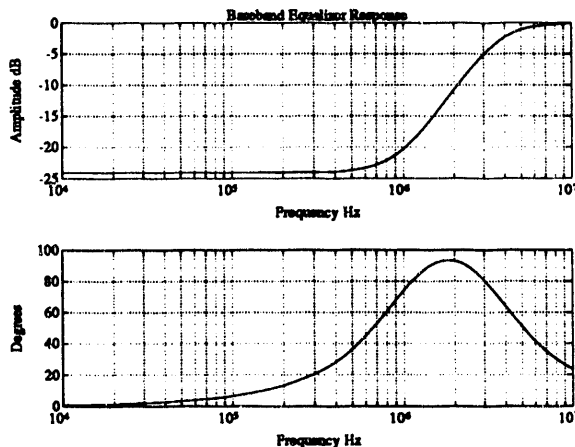


Figure 11: Baseband equalizer response

Realization of the filter response was achieved using state space techniques. The MATLAB function TF2SS was used to make the transformation into control canonical form. Figure 12 shows the general form for state space representation of a transfer function. Figure 13 populates the matrixes with values

consistent with the equalizer filter.

$$\begin{bmatrix} X_1 \\ X_2 \end{bmatrix} = \begin{bmatrix} A \\ B \end{bmatrix} \begin{bmatrix} X_1 \\ X_2 \end{bmatrix} + \begin{bmatrix} B \\ D \end{bmatrix} \text{input}$$

$$\text{output} = \begin{bmatrix} C \\ D \end{bmatrix} \begin{bmatrix} X_1 \\ X_2 \end{bmatrix} + \begin{bmatrix} D \\ D \end{bmatrix} \text{input}$$

Figure 12: General state space transfer function

$$A = \begin{bmatrix} -3.52 \times 10^7 & -6.17 \times 10^{14} \\ 1 & 0 \end{bmatrix} \quad B = \begin{bmatrix} 1 \\ 0 \end{bmatrix}$$

$$C = \begin{bmatrix} -2.64 \times 10^7 & -5.79 \times 10^{14} \end{bmatrix} \quad D = \begin{bmatrix} 1 \end{bmatrix}$$

Figure 13: Matrix values for equalizer function

To make the gains in the C matrix more reasonable, the following substitution is made:

$$X_1 = \frac{1}{2.64 \times 10^7} Z_1 \quad Z_1 = [2.64 \times 10^7] X_1$$

$$X_2 = \frac{1}{5.79 \times 10^{14}} Z_2 \quad Z_2 = [5.79 \times 10^{14}] X_2$$

Figure 14: Substitution values

The resulting relationship (figure 15) has two -1 entries in the C matrix which can easily be implemented with an op-amp summing node.

$$\begin{bmatrix} Z_1 \\ Z_2 \end{bmatrix} = \begin{bmatrix} -3.52 \times 10^7 & -2.81 \times 10^7 \\ 2.19 \times 10^7 & 0 \end{bmatrix} \begin{bmatrix} Z_1 \\ Z_2 \end{bmatrix} + \begin{bmatrix} 2.64 \times 10^7 \\ 0 \end{bmatrix} \text{input}$$

$$\text{output} = \begin{bmatrix} -1 & -1 \end{bmatrix} \begin{bmatrix} Z_1 \\ Z_2 \end{bmatrix} + \begin{bmatrix} 1 \end{bmatrix} \text{input}$$

Figure 15: Matrixes after substitution

The next step is to transform the matrix representation into the Laplace domain. Here differentiated elements are operated on by  $s$ , the Laplace operator.

$$\begin{bmatrix} sZ_1 \\ sZ_2 \end{bmatrix} = \begin{bmatrix} -3.52 \times 10^7 & -2.81 \times 10^7 \\ 2.19 \times 10^7 & 0 \end{bmatrix} \begin{bmatrix} Z_1 \\ Z_2 \end{bmatrix} + \begin{bmatrix} 2.64 \times 10^7 \\ 0 \end{bmatrix} [input]$$

Figure 16: Laplace representation of the two states

Figure 16 contains two equations of the form:

$$sZ_1 = A_{11}Z_1 + A_{12}Z_2 + B_1[input]$$

Figure 17: An equation defining state  $Z_1$

If we divide the two equations having the form illustrated in figure 17 by  $s$ , the resulting relationship can be realized with a single op-amp circuit. Recall that an integrator has the following transfer function:

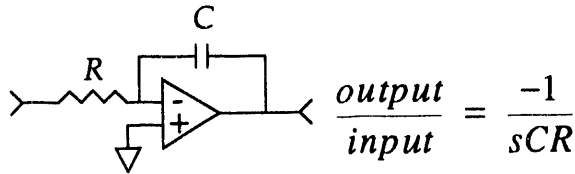


Figure 18: Op-amp integrator circuit

If one studies the matrix relations, it becomes clear that the transfer function can be realized with a total of five op-amps. Two amps are configured as integrators to implement the equations of figure 17, two are needed for inversion, and the last is used to sum the two states and the inverted input to create the output. Figure 19 shows this realization.

Calculating the component values is simply a matter of choosing a reasonable value for the integrator capacitors and equating the time constant of each integrator input to the corresponding coefficient from the state

equations. Figure 20 contains these results.

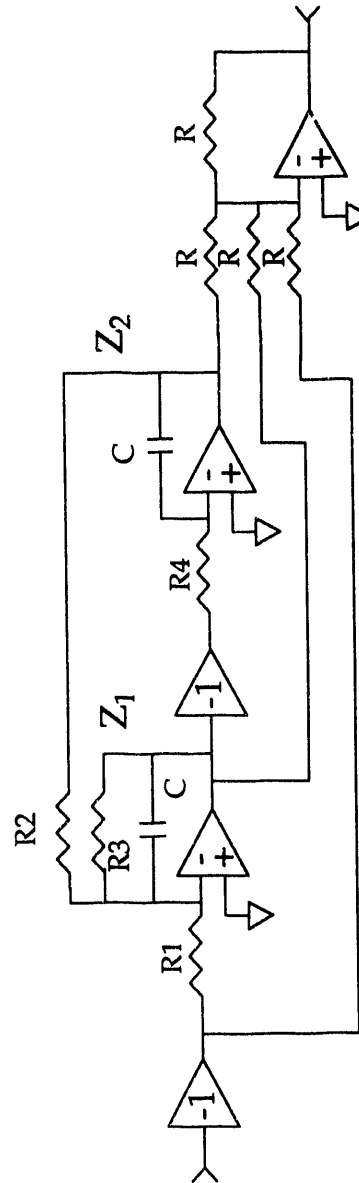


Figure 19: Schematic of filter

Selection of a good op-amp is important. Since the filter response extends to several MHz, a wideband amplifier is needed. Current feedback op-amps offer large bandwidths but are not stable for integrator applications. This application calls for a voltage feedback op-amp which is stable at unity gains. We selected an impressive device from Elantec, the EL2073. This amplifier has a 200 MHz

gain-bandwidth product, and is unity gain stable as required. Spice simulation using an ideal op-amp matched the measured filter response except for 5 ns of additional delay.

$$\frac{1}{sCR_1} = \frac{B_1}{s} = \frac{2.64 \times 10^7}{s} \quad R_1 = \frac{1}{C \times 2.64 \times 10^7}$$

$$\frac{1}{sCR_2} = \frac{A_{12}}{s} = \frac{2.81 \times 10^7}{s} \quad R_2 = \frac{1}{C \times 2.81 \times 10^7}$$

$$\frac{1}{sCR_3} = \frac{A_{11}}{s} = \frac{3.52 \times 10^7}{s} \quad R_3 = \frac{1}{C \times 3.52 \times 10^7}$$

$$\frac{1}{sCR_4} = \frac{A_{21}}{s} = \frac{2.19 \times 10^7}{s} \quad R_4 = \frac{1}{C \times 2.19 \times 10^7}$$

Figure 20: Calculating resistor values

Resistor	Value
R1	379 ohms
R2	356
R3	284
R4	457

Table 1: Results assuming C = 100 pF

Figure 21 shows the actual measured 500 kW PEP-II klystron transfer function. Figure 22 is the response of the equalizer filters including the RF circuitry to mix down and back up to 476 MHz. The measured group delay is -190 ns at 476 MHz. Finally figure 23 is the cascaded response of the klystron and the equalizer filter. The cascaded group delay at 476 MHz has been reduced to 82 ns. MATLAB calculations show that the addition of the equalizer allows for 6 dB additional loop gain

and doubles the loop bandwidth.

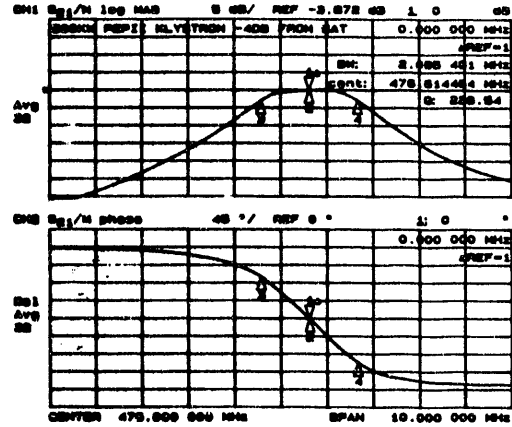


Figure 21: Measured klystron response

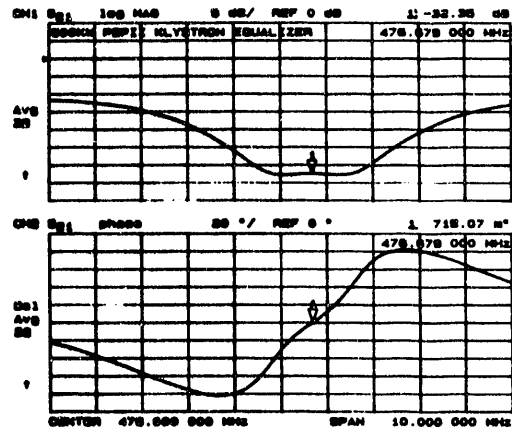


Figure 22: Measured equalizer response

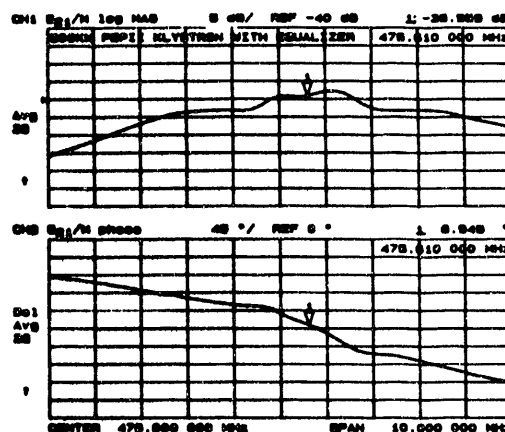


Figure 23: Measured klystron-equalizer response

## 6. CONCLUSIONS

Large group delays common in today's high power klystron tubes used for storage rings can be effectively compensated for. We have demonstrated a technique which is technically very feasible, low cost and effective.

Matching the equalizer response to a particular klystron may require some iteration, but this is just a matter of optimization. One could consider an adaptive method to tailor the combined response to a model filter (analog or digital). Figure 24 should be considered "food for thought".

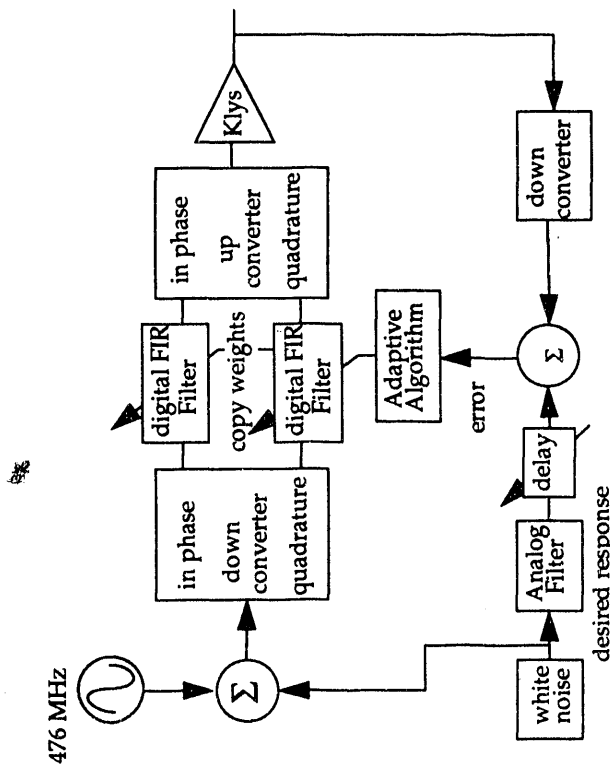


Figure 24: Adaptive klystron equalizer

## 7. THANKS

Thanks to the following people at SLAC who assisted in this development:

Greg Dalit  
John Fox  
Haitham Hindi  
Heinz Schwarz

Special thanks to Flemming Petersen of CERN who both inspired and contributed to this project.

## 8. REFERENCES

1. R. A. Rimmer, **RF Cavity Development for the PEP-II B Factory**, These proceedings (1993).
2. J. D. Fox, et al., **Multibunch Feedback - Strategy, Technology and Implementation Options**, SLAC-PUB-5957 (1992).
3. H. Hindi, et al., **Down Sampled Signal Processing for a B Factory Bunch-by-Bunch Feedback System**, Proceedings of the Third European Particle Accelerator Conference, Berlin, Germany. p. 1067 (1992).
4. **PEP-II, An Asymmetric B Factory Design Update**, Conceptual Design Report Update, LBL PUB-5303, SLAC-372 (1992).
5. F. Petersen, **Multibunch Instabilities**, Transparencies from Joint US-CERN Accelerator School, Benalmadena Spain (1992).
6. F. Petersen, **RF Cavity Feedback**, Internal SLAC Report, (1992).
7. G. Lambertson, **Effective Impedances from the Fundamental Mode**, BECON-100 (1991).



**END**

---

**DATE  
FILMED  
3/19/93**

